Rev. Roum. Sci. Techn.– Électrotechn. et Énerg.
Vol. **70**, *3*, pp. 376–384, Bucarest, 2025

HYBRID DESIGN PATCH ANTENNA FOR X-BAND SATELLITE COMMUNICATION

MOHAMMED ZAKARYA BABA-AHMED[1], RAHMA DJAOUDA TALEB[2], MOHAMMED AMIN RABAH[3], SIDAHMED BENABBOU[4], MERIEM IKRAM SOUFI[5]

Keywords: Antenna arrays; Design optimization; Patch antennas; X-band frequencies; Satellite communication.

This study presents a novel approach to the development and application of a rectangular patch antenna optimized for X-band satellite communication operations. The antenna's performance is enhanced through geometry refinement and the strategic introduction of slots. A novel hybrid design is proposed, combining series and parallel patch antenna arrays in a four-element structure to improve gain, impedance matching, and directivity. These findings offer practical implications for satellite applications, spanning areas such as radar systems, telecommunications, and diverse radio wave applications, including cognitive radio. The simulation and measurement results show a close resemblance for both resonance frequencies at 9.5 GHz, indicating acceptable matching. In terms of the measured S11, two resonance frequencies with excellent matching at 9.018 GHz (S11 = -34.45 dB) and 10.31 GHz (S11 = -21.2 dB). On the other hand, for the simulated S11, there is a resonance frequency at 9.5 GHz with good matching and an S11 value of -35.8 dB. These results indicate that our implemented antenna network is multi-resonant, demonstrating satisfactory matching for multiple frequencies within the X-band with only one antenna array.

1. INTRODUCTION

Antenna networks and reconfigurable antennas represent dynamic areas of focus in antenna design research. Antenna networks comprise multiple antennas that collaborate to create specific radiation patterns, with applications in radar systems, wireless communication, and satellite navigation [1,2]. On the other hand, reconfigurable antennas possess the capability to modify their electromagnetic characteristics in response to external control signals [3,4]. This adaptability enables them to optimize performance across diverse electromagnetic environments [5].

Various techniques, including adjustments to antenna geometry, operating frequency, and material properties, can be employed to achieve reconfigurable antennas [6–8]. The combination of antenna networks and reconfigurable antennas offers flexibility and adaptability to changing environments, making them essential in navigation, surveillance, and communication systems, such as cognitive radio systems [9]. Cognitive radios' adaptability enables them to operate across diverse frequency bands, thereby enhancing spectrum resource utilization and facilitating coexistence among wireless systems [10,11].

Patch antennas' reconfigurability addresses limitations by enabling real-time adjustments to characteristics such as operating frequency, radiation pattern, polarization, and shape [12]. This dynamic adaptability empowers patch antennas [13] to effectively meet changing channel conditions, spatial coverage requirements, and user needs. The result is a substantial improvement in overall performance, particularly for satellite communication systems [14].

This paper presents a comprehensive study on the design, simulation, and implementation of a reconfigurable rectangular patch antenna array for use in X-band satellite communication.

2. DESIGN OF THE RECTANGULAR PATCH ANTENNA

This section delves into the geometry of the simulated antenna and its tuning for optimal performance at the target frequency of 9.5 GHz. It outlines the incorporation of notches and adjustments to the patch width, providing a detailed account of the modifications made to enhance matching characteristics.

2.1 DESIGN OF THE RECTANGULAR PATCH ANTENNA

The suggested antenna is a rectangular patch antenna resonating at 9.5 GHz, engineered for impedance matching to 50 Ω. It is crafted with an FR-4 type (LOSSY) substrate, featuring a relative permittivity (ε_r) of 4.3 and a thickness (h) of 1.6 mm, Fig. 1. The ground plane is constructed from the same material as the patch (Copper) and maintains an identical thickness (t) of 0.035 mm.

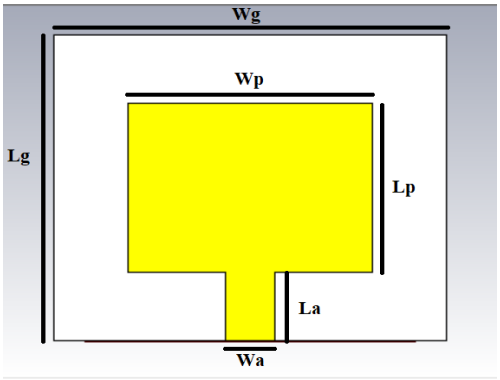

Fig. 1 – Structure of a simple rectangular patch.

The antenna dimensions were determined using the equations [15–17] outlined in Table 1:

Table 1

Parametric equations for a rectangular patch antenna.

Antenna Parameters	*Equations*
Actual patch length	$L_p = L_{eff} - 2\Delta l$ (1)
Effective length	$L_{eff} = \frac{c}{(2f_r\sqrt{\varepsilon_{reff}})}$ (2)
Length extension	$\Delta l = \frac{(0.412h(\varepsilon_{reff}+0.3)(w/h+0.264))}{((\varepsilon_{reff}-0.258)(w/h+0.8))}$ (3)

[1,2,3,4,5] Department of Telecommunication, Faculty of Technology, University of Abou-Bekr Belkaid of Tlemcen, Laboratory of Telecommunication of Tlemcen (LTT), Tlemcen, Algeria.
[1] Faculty of Technology of the University of Hassiba Ben Bouali of Chlef, Chlef, Algeria.
[3] Algerian Space Agency Satellite Development Center, Oran, Algeria.
E-mails: mohammedzakarya.baba-ahmed@univ-tlemcen.dz, rahmadjaouda.taleb@univ-tlemcen.dz, mohammedamin.rabah@univ-tlemcen.dz, sidahmed.benabbou@univ-tlemcen.dz, meriemikram.soufi@univ-tlemcen.dz

DOI: 10.59277/RRST-EE.2025.70.3.16

Dielectric constant	$\varepsilon_{reff} = \frac{(\varepsilon_r+1)}{2} + \frac{(\varepsilon_r-1)}{2}\left[1 + 12\frac{h}{w}\right]^{-1/2}$ (4)
Patch width	$W_p = \frac{c}{\left(2f_r\sqrt{(\varepsilon_r+1)}\right)}$ (5)
Substrate length	$L_s = L_p + 6h$ (6)
Substrate width	$W_s = L_s + 6h$ (7)
Line width	$W_f = \frac{8e^A}{e^{2A-2}} \times h$ (8)
	With
	$A = \frac{Z\sqrt{(2(\varepsilon_r+1)}}{120} + \frac{1}{2} + \frac{(\varepsilon_r-1)}{(\varepsilon_r+1)} + \left(h\,ln\frac{\pi}{2} + \frac{1}{\varepsilon_r} \times ln\frac{4}{\pi}\right)$

The results of the calculations are presented in Table 2.

Table 2

Dimensions of the proposed rectangular patch antenna.

Parameters	Dimensions
W_g	22 mm
L_g	18.52 mm
W_p	9.69 mm
L_p	6.92 mm
W_a	3.13 mm
L_a	5.8 mm
h	1.6 mm
T	0.035 mm

2.2 NEW ANTENNA STRUCTURE

At this stage, modifications were made by adding notches with a width of gpf = 0.5 mm and a length of fi = 2.11 mm. Additionally, the patch width was increased after a parametric study using the software (Wp = 11.27 mm) to achieve resonance at the desired frequency (9.5GHz). In this phase, we introduce apertures in the form of slots, each having a width (We) of 0.5 mm and a length (L) of 1 mm. These slots are spaced at intervals of a = 0.5 mm, as illustrated in Fig. 2.

The Computer Simulation Technology (CST) Microwave Studio is employed for the 3D simulation of high-frequency components, making it ideal for our antenna design. Its versatility and effectiveness in handling various homogeneous structures ensure accurate results [18].

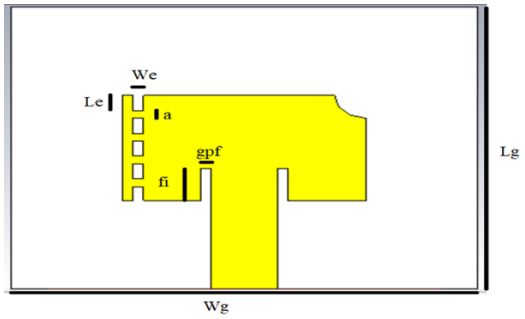

Fig. 2 – The new antenna structures.

The S_{11} parameter serves as a key metric for evaluating antenna performance, with a lower value indicating better impedance matching between the antenna and the system [19].

Following the incorporation of the slots, a favorable match at a frequency of 9.5 GHz has been achieved, resulting in a reflection coefficient (S_{11}) of -17.23 dB.

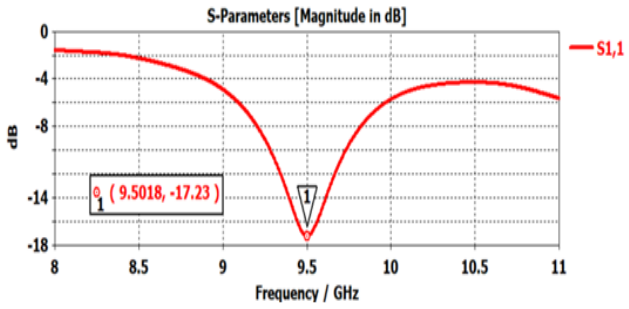

Fig. 3 – Reflection coefficient of the new structure.

The voltage standing wave ratio (VSWR) is less than 2, precisely at 1.61. A low VSWR signifies that the antenna is well-matched to the transmission line, indicating efficient power transfer from the transmission line to the antenna [20,21].

Figure 4 illustrates the antenna gain across different frequencies. At 9.5 GHz, the antenna exhibits a positive gain of 2.9 dBi.

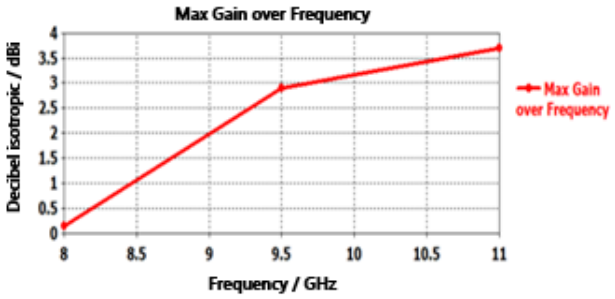

Fig. 4 – Maximum gain at 9.5 GHz.

3. NOVEL HYBRID RECONFIGURABLE DESIGN PATCH ANTENNA IN X-BAND

In contemporary wireless communication networks, the demand for antennas capable of operating across a wide range of frequencies has intensified. In response to this need, reconfigurable antennas are employed to mitigate costs associated with intricate hardware and systems. The augmentation of radiating elements offers the potential for achieving heightened gain, improved adaptability, or a combination of both attributes. Consequently, in this section, we explore the design of antenna arrays in parallel, series, and hybrid configurations, incorporating two and four elements. The objective of these designs is to investigate the potential enhancements they can bring to X-band satellite communications and reconfigurable antennas.

3.1 DESIGN OF A TWO-ELEMENT PARALLEL

In this section, we introduce the design of a two-element parallel antenna array in Fig. 5 and the design of a two-element series antenna array in Fig. 6.

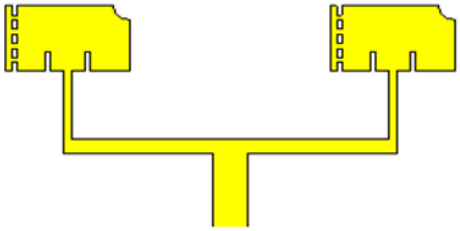

Fig. 5 – Structure of a two-element parallel antenna array.

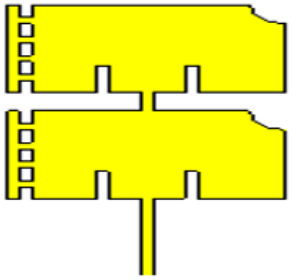

Fig. 6 – Structure of a Two-Element Series Antenna Array.

The series antenna element is fed with a 50 Ω impedance. Therefore, the starting point of the feed line in the parallel antenna will be 50 Ω, followed by a 75 Ω line, and the input impedance of the two patches will be 100 Ω.

3.2 ANALYSIS AND COMPARISON BETWEEN A TWO-ELEMENT SERIES AND A PARALLEL

In this section, we present the simulation results for the reflection coefficient (S_{11}) and the gain of the series and parallel designs of the two-element antenna array.

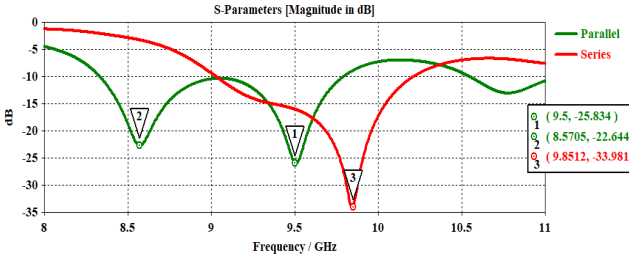

Fig. 7 – Comparison between the reflection coefficient of a two-element series and parallel antenna array.

Figure 7 illustrates the reflection coefficient S_{11} of a parallel antenna array, measuring -25.83 dB at the resonant frequency of 9.5 GHz and -22.64 dB at 8.57 GHz, and the reflection coefficient S11 of a series antenna array measuring -33.98 dB at the resonant frequency of 9.85 GHz.

While the serial antenna array achieves excellent antenna adaptation [22] at -33.98 dB, this occurs at a different resonant frequency of 9.85 GHz. The parallel design exhibits suboptimal performance with a reflection coefficient of -25.83 dB, but performs better at the desired frequency of 9.5 GHz, indicating good impedance matching at the target frequency.

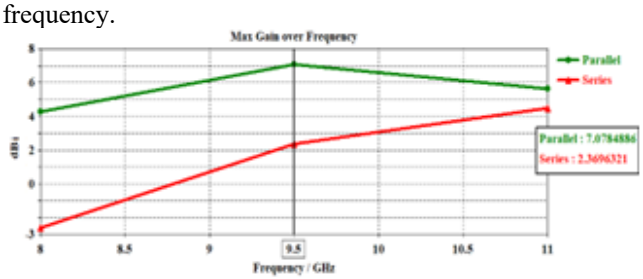

Fig. 8 – Comparison between the maximum gain of a two-element series and parallel antenna array at 9.5 GHz frequency.

Figure 8 shows that the parallel antenna array achieves a maximum gain of 7.07 dBi at the resonant frequency of 9.5 GHz, which is significantly higher than the gain of the series antenna array, which measures only 2.36 dBi at the same frequency. This demonstrates that the two-element parallel design [23] offers superior performance in terms of gain compared to the series design at 9.5 GHz.

4. DESIGN OF A FOUR-ELEMENT HYBRID ARRAY

In this section, we introduce the design and analysis of a Four-Element Hybrid antenna network. The objective is to enhance both gain and S11 parameters by utilizing reconfigurable antenna arrays. The article outlines the design and simulation of two-element parallel and series configurations, aiming to leverage the advantages of each design. Subsequently, a four-element hybrid configuration is introduced, combining the strengths of both parallel and series designs. The discussion emphasizes the benefits of these configurations over a single antenna. The design of the antenna array shown in Fig. 9 utilizes the exact dimensions provided in Table 2.

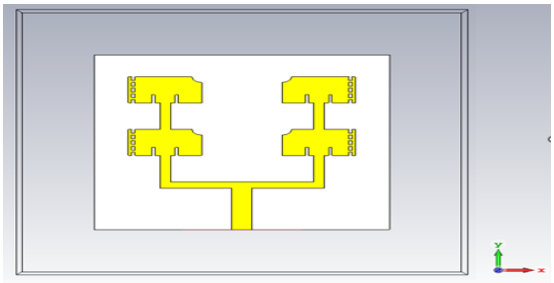

Fig. 9 – Network structure of four elements in a hybrid power supply.

The results obtained from simulations are presented and discussed in this section, encompassing key parameters such as reflection coefficient, voltage standing wave ratio (VSWR), radiation pattern, and gain. The analysis examines the impact of Hybrid design reconfigurability on antenna performance, offering insights into how the introduced configurations affect the overall behavior and effectiveness of the antenna system.

As illustrated in Fig. 10, the structure of the four-element hybrid antenna network demonstrates outstanding adaptation, exhibiting an S11 of -35.8 dB precisely at the required frequency.

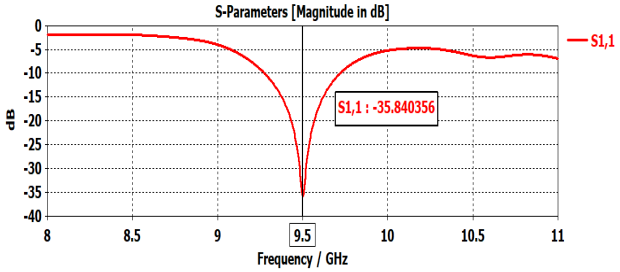

Fig. 10 – Reflection coefficient of the new hybrid structure.

As depicted in Fig. 11, the voltage standing wave ratio (VSWR) is recorded at 1.03, which is less than 2. This indicates that the antenna is accurately matched to the desired frequency.

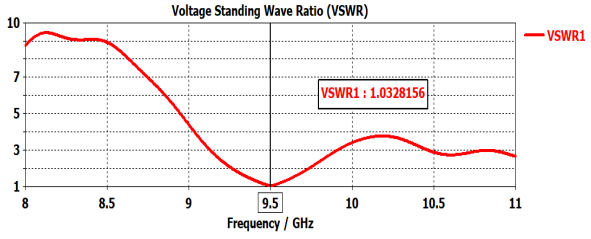

Fig. 11 – VSWR of a four-element series antenna network with hybrid feeding.

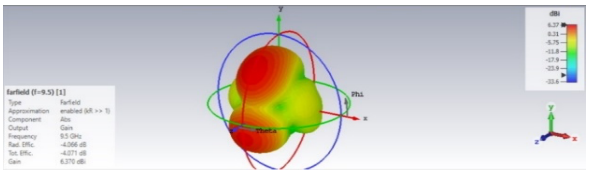

Fig. 12 – Radiation pattern of the hybrid antenna at 9.5 GHz in 3D.

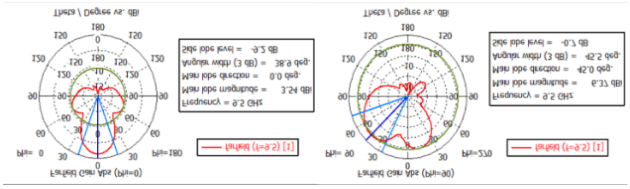

Fig. 13 – Radiation pattern (phi = 0° and 90°) of the hybrid antenna at 9.5 GHz in 2D.

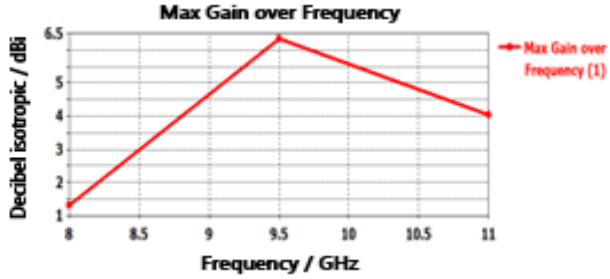

Fig. 14 – Gain of hybrid design at 9.5 GHz.

The mentioned results emphasize that the hybrid four-element array demonstrates a significant improvement in adaptation, achieving -35.84 dB, which is similar to that of the series' two-element array. Additionally, there is an increase in gain, measured at 6.376 dBi at f = 9.5 GHz, which is identical to that of the two parallel elements. Consequently, it can be inferred that the hybrid antenna array enhances both matching and gain compared to the basic single-element antenna. The antenna exhibits directivity, with a numerical aperture of 38.9 degrees at phi = 0 ° and 45.5 degrees at phi = 90 °.

4.1 COMPARISON RESULTS

Table 3 provides a comparative summary for all results.

Table 3

Concise comparison of the results for the various antenna structures at 9.5 GHz

Structure of Antenna	S11 (dB)	Gain (dBi)	Dimensions (cm²)
Single Antenna	-12.52	2.90	4.07
Two-Element Parallel	-25.83	7.07	15.28
Two-Element Series	-33.98	2.36	5.80
Hybrid Antenna	-35.84	6.35	21.27

According to this comparison, the four-element hybrid antenna array stands out as the most favorable configuration, delivering the best results for both the S11 parameter and the VSWR. It achieves a remarkable adaptation of -35.84 dB and a VSWR of 1.03, with dimensions of 21.27 cm². This is reasonable since the structure combines the dimensions of both the series and parallel configurations. Additionally, the network gain of the hybrid antenna is 6.35 dBi, which, while slightly less than the best result obtained from the two elements in parallel, remains highly commendable. In summary, based on these results, it can be concluded that the hybrid antenna array offers an excellent overall solution, effectively improving multiple parameters in a structurally reconfigurable antenna.

5. EXPERIMENTAL RESULTS

After the completion of the antenna arrays on both the upper and lower surfaces by the company ALMITECH located in Kouba, Algiers, Algeria, we proceeded with the assembly of the hybrid antenna array. To accomplish this, we conducted the soldering of SMA type connectors at designated locations to facilitate the excitation of the antennas.

Reflection coefficient measurements of the antenna networks were conducted using the Agilent PNA (Network Analyzer) model N5222A at the Instrumentation and Metrology-AIT laboratory in the Assembly, Integration, and Test department of the Satellite Development Center in Oran. This two-port equipment enables measurements in the frequency range of 10 MHz to 26.5 GHz, with calibration performed between 2 and 3 GHz. The networks were characterized while connected using SMA-type coaxial cables. The following Figures respectively depict photographs, results, and comparisons of the four-element antenna arrays in a hybrid new design configuration.

5.1 THE ANTENNA NETWORK WITH HYBRID DESIGN

In the context of our study, we investigated the antenna network with a hybrid feed configuration.

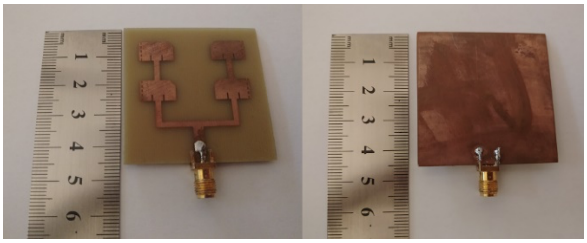

Fig. 15 – The Implemented Hybrid Antenna Network

5.2 Measurement of Reflection Coefficients and Voltage Standing Wave Ratio (VSWR)

The measurement setup for the antenna network is depicted in the following Fig. 16.

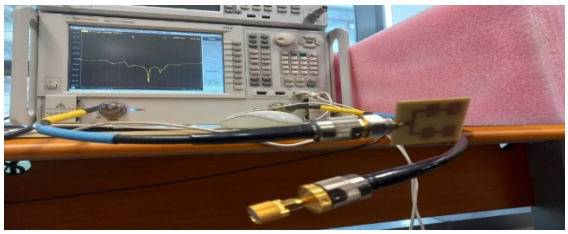

Fig. 16 –Testing the Hybrid Antenna Network

After the test, the following results are shown in Fig. 17.

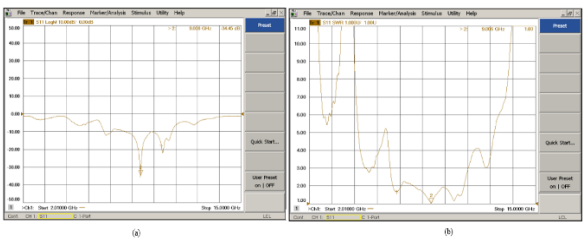

Fig. 17 – (a) Measured Reflection Coefficient S11 and (b) Voltage Standing Wave Ratio (VSWR) of the Hybrid Antenna Array.

A comparison was conducted between the results obtained from the analyzer and those from the electromagnetic simulation after exporting the analyzer results. Fig. 18 illustrate the comparison between simulation and measurements for the hybrid antenna array.

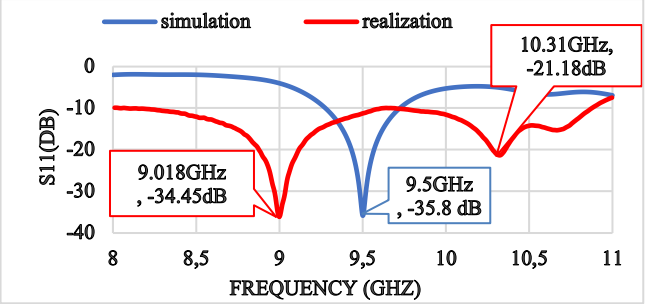

Fig. 18 – Comparison between the simulated and measured reflection coefficient of a hybrid antenna array.

According to Fig. 18, the simulation and measurement results show a close resemblance for both resonance frequencies at 9.5 GHz, indicating acceptable matching. In terms of the measured S11, two resonance frequencies are observed with excellent matching at 9.018 GHz (S_{11} = -34.45 dB) and 10.31 GHz (S11 = -21.2 dB). On the other hand, for the simulated S11, there is a resonance frequency at 9.5 GHz with good matching and an S11 value of -35.8 dB. These results indicate that our implemented antenna network is multi-resonant, demonstrating satisfactory matching for multiple frequencies within the X-band, with only one antenna array. This is an advantage compared to the study made in the reference [24]. The experimental results identified a multi-resonance, like that in the two-element series and parallel antenna array, which was not initially captured in the hybrid antenna simulation. This finding proves beneficial for the reconfigurability of the four-element hybrid antenna. The ability to identify and leverage multi-resonance in the experimental results contributes to a more comprehensive understanding and optimization of the antenna system.

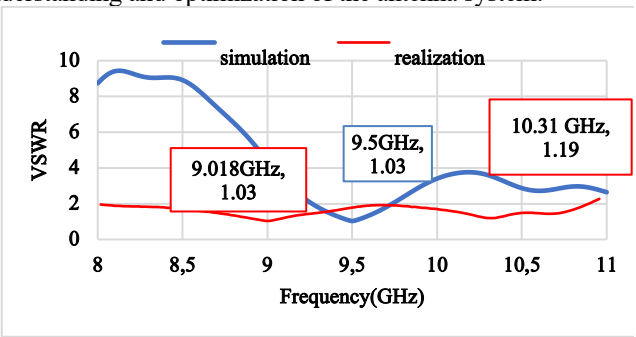

Fig. 19 Comparison of simulated and measured VSWR of the antenna array.

It is observed in Fig. .19 that the VSWR falls between 1 and 2 at both frequencies, 9.018 GHz and 9.5 GHz, indicating good matching between the antenna and the transmission line.

Upon analyzing Figs. 18 and 19, a slight frequency shift in the bandwidths of the hybrid antenna network is noticed. It is worth noting that the measurement results are in satisfactory agreement with the simulated results. Furthermore, the measured and simulated bandwidths are nearly identical. This observation demonstrates significant consistency between the experimentally obtained values and those predicted by simulations. However, the slight deviation between simulation and measurements could be attributed to manufacturing defects and/or measurement uncertainties. Despite these discrepancies, the measurement results for the hybrid antenna align well with the specifications outlined in our requirements document.

The results obtained will enable us to study the reconfigurability of the antenna in various aspects, including PIN diodes, MEMS, and antenna matching, as mentioned in [25, 26], as well as with other technologies that leverage reconfigurability, such as cognitive radio [27].

5.3 COMPARISON WITH RECENT WORKS

Table 4 compares the performance characteristics of the proposed antenna array to those of other previous works.

Table 4

A comparison of the suggested antenna and some published studies.

References	X-Band Frequency (GHz)	S11 (dB)	Gain (dBi)	VSWR
[28]	9.49	-24.11	3.84	/
[29]	7.17;8.3;10.82; 11.3	-30; -22; -28; -35	1.7; 3.61; 4.01; 3.81	1.06;1.16; 1.08;1.04
[30]	8.5;11.1	-10.79; -20.43	2.49; 3.84	/
References	X-Band Frequency (GHz)	S11 (dB)	Gain (dBi)	VSWR
[31]	10.8; 11.1 9.7	-12.4; -21.34	6.29; 5.5	1.31; 1.98
[32]	9.5	-26.5	5	/
Our hybrid antenna array		-35.84	6.35	1.03

Table 4 provides valuable insights into antenna performance across operating frequencies, reflection coefficient (S11), maximum gain, and VSWR. Previous references exhibit divergent measurements across different antenna types, all operating on reconfigurable antennas within the X-band. However, our reconfigurable hybrid antenna stands out by achieving an impressive -35.84 dB for minimal reflection at a resonance frequency of 9.5 GHz, coupled with a remarkable maximum gain of 6.35 dBi and an ideal VSWR of 1.03. These results underscore the substantial potential of our hybrid antenna array in satellite applications that necessitate the utilization of the X-band.

5. CONCLUSION

The current study focuses on simulating a reconfigurable printed antenna array for X-band satellite communications at a frequency of 9.5 GHz. Various modifications, including enhancements to the frequency reconfigurable structure, were implemented with the overarching objective of creating a reconfigurable printed hybrid antenna optimized for satellite applications.

Using CST software, three reconfigurable patch antenna networks were designed: a two-element antenna network (series and parallel) and a four-element hybrid antenna network. All reflection coefficients are below -10 dB, and gains exceed 3 dB.

All the proposed antennas were designed using CST software, ensuring they met the requirements of satellite applications. The antenna demonstrates the capability to

change its resonance frequency in the X-band for diverse applications. Finally, the implementation and measurements of the hybrid antenna network were conducted to validate the simulated results, contributing to the better optimization of printed antennas in the X-band for various satellite applications.

CREDIT AUTHORSHIP CONTRIBUTION STATEMENT

Mohammed Zakarya Baba-Ahmed: Writing - conceptualization
Rahma Djaouda Taleb: Formal analysis and investigation
Mohammed Amin Rabah: Methodology
Sidahmed Benabbou: Writing - original draft preparation
Ikram Meriem Soufi: Review and editing

Received on 7 August 2024

REFERENCES

1. Z. Xiao, Z. Han, A. Nallanathan, O.A. Dobre, B. Clerckx, J. Choi, C. He, W. Tong*, Antenna array enabled space/air/ground communications and networking for 6G,* IEEE Journal on Selected Areas in Communications, **40**, *10*, pp. 2773–2804 (2022).
2. P. Prasad, S.N. Singh, A. Kumar, *Lightweight ultra-wideband antenna array equipped with thin frequency selective surface for high-gain applications,* Journal of Electrical Engineering**, 73,** *6*, pp. 396–404 (2022).
3. Z. Zhang, H. Shi, L. Wang, J. Chen, X. Chen, J. Yi, A. Zhang, H. Liu, *Recent advances in reconfigurable metasurfaces: Principle and applications,* Nanomaterials, **13**, *3*, pp. 534 (2023).
4. D.N. Gençoğlan, M. Palandöken,, Ş. Çolak, *Novel frequency-reconfigurable antennas with ring resonators and RF switches: enhancing versatility and adaptability in wireless communication systems*, Applied Sciences, **13**, *18,* pp. 10237 (2023).
5. V. Nath, *Frequency reconfigurable circular microstrip G-slotted antenna with DGS for various wireless applications*, International Journal of Microwave and Wireless Technologies, **16,** *3*, pp. 505–514 (2024).
6. S.K. Muthuvel, Y.K. Choukiker, *Wideband frequency agile and polarization reconfigurable antenna for wireless applications*, IETE Journal of Research, **69,** *3*, pp. 1529–1538 (2023).
7. K. Karthika, K. Kavitha, *Reconfigurable antennas for advanced wireless communications: A review*, Wireless Personal Communications, **120,** *4*, pp. 2711–2771 (2021).
8. R.D. Taleb, M.Z. Baba-Ahmed, F. Bousalah, M.A. Rabah, *Reconfigurable and ecological intelligent antenna for satellite communication*, International Conference on Artificial Intelligence in Renewable Energetic Systems, pp. 415–426 (2022).
9. M.Z. Baba-Ahmed, S. Tahraoui, A. Sedjelmaci, M. Bouregaa, M.A. Rabah, *Self-management of autonomous agents dedicated to cognitive radio networks*, In Smart Energy Empowerment in Smart and Resilient Cities: Renewable Energy for Smart and Sustainable Cities, Springer, pp. 451–464 (2020).
10. G. Mackertich-Sengerdy, S.D. Campbell, P.L. Werner, D.H. Werner, *Ruggedized reconfigurable antennas through the implementation of innovative mechanical techniques,* International Applied Computational Electromagnetics Society Symposium (ACES), Monterey, CA, USA, March 26-30 (2023).
11. N. Seghiri, M.Z. Baba-Ahmed, B. Benmammar, N. Houari, M.K. Khellafi, M.A. Abdelgherfi, *Data security of a cognitive radio network for multicriteria secondary users*, Journal of Electrical and Electronics Engineering, **15**, *2*, pp. 82–87 (2022).
12. K. Ramahatla, M. Mosalaosi, A. Yahya, B. Basutli, *Multiband reconfigurable antennas for 5G wireless and CubeSat applications: A review*, IEEE Access, **10,** pp. 40910–40931 (2022).
13. C. Ferchichi, D. Omri, T. Aguili, *Utilizing 1D convolutional neural networks for enhanced design and optimization of rectangular patch antenna parameters*, IEEE International Symposium on Networks, Computers and Communications (ISNCC), Istanbul, Turkey, Oct. 23, pp. 1–6 (2023).
14. L. Xie, L. Chi, B. Lin, X. Wang, Y. Qi*, A compact channel patch antenna with reconfigurable circularly polarized pattern for mobile satellite communications*, AEU-International Journal of Electronics and Communications, **164,** pp. 154632 (2023).
15. H.M. Marhoon, N. Qasem, *Simulation and optimization of tunable microstrip patch antenna for fifth-generation applications based on graphene*, International Journal of Electrical and Computer Engineering (IJECE), **10**, *5*, pp. 5546–5558 (2020).
16. H.M. Marhoon, H.A. Abdulnabi, Y.Y. Al-Aboosi, *Designing and analyzing of a modified rectangular microstrip patch antenna for microwave applications*, Journal of Communications, **17**, *8*, pp. 668-674 (2022).
17. F.A. Ningrum, S. Muliyani, F. Fadjrianah, M.R. Effendi, A. Munir, *Proximity-Coupled Ku-Band patch array antenna for imaging application*, IEEE International RF and Microwave Conference (RFM), IEEE, Penang, Malaysia, Nov. 14-16, pp. 1–5 (2022).
18. A.K. Al-Azzawi, *New design approach of a "2.4 GHz" slotted rectangular patch antenna with a wideband harmonic suppression*, Arabian Journal for Science and Engineering**, 46,** pp. 1–10 (2021).
19. A. Baz, D. Jansari, S.P. Lavadiya, S.K. Patel, *Miniaturized and high gain circularly slotted 4×4 MIMO antenna with diversity performance analysis for 5G/Wi-Fi/WLAN wireless communication applications*, Results in Engineering, **20**, pp. 100185 (2023).
20. A.H. Murshed, MA. Hossain, M.A. Rahman, E. Nishiyama, I. Toyoda, *Design and characterization of polarization reconfigurable heart shape monopole antenna for 2.4 GHz application,* International Journal of Electrical and Computer Engineering, **12***, 4*, pp. 3808–3817 (2022).
21. X.P. Li, C.J. Duan, G. Xu, M.M. Li, L. Yan, W. Li, *Compact broadband bi-directional circularly polarized fan-shaped patch with parasitic annular groove for S-band satellite applications*, International Journal of RF and Microwave Computer-Aided Engineering, **32**, *11* (2022).
22. B.G. Hakanoglu, B. Koc, O. Sen, H. Yalduz, M. Turkmen, *Stub loaded patch antenna and a new approach to size reduction for sub-6 GHz 5G and Wi-Fi frequencies*, Advances in Electrical & Computer Engineering**, 21**, *2* (2021).
23. P. Gupta, M. Bharti, A. Kumar, *Circular polarized two-element compact dual-band MIMO antenna for 5G and wearable applications*, Rev. Roum. Sci. Techn. – Électrotechn. Et Énerg., **67**, *3*, pp. 321–326 (2022).
24. A. Basgumus, M. Namdar, T. Tsiftsis, *Broadcast cognitive radio with dirty paper coding over Nakagami-m fading channel*, Advances in Electrical and Computer Engineering, **19,** *1*, pp. 3–8 (2019).
25. N. Kiani, F. Tavakkol Hamedani, P. Rezaei, *Design of an ultra-compact reconfigurable IDC graphene-based SIW antenna in THz band with RHCP*, Telecommunications Systems (2024).
26. T. Tandel, S. Trapasiya, *Reconfigurable antenna for wireless communication: Recent developments, challenges and future*, Wireless Personal Communications (2023).
27. D.V. Niture, S P. Mahajan, *A compact reconfigurable antenna for UWB and cognitive radio applications*, Wireless Personal Communications, **125**, pp. 3661–3679 (2022).
28. D. Kumar, A.S. Siddiqui, H.P. Singh, M.R. Tripathy, W.U.H. Paul, *Design and implementation of reconfigurable frequency and polarization microstrip patch antenna for X-Band application*, Tuijin Jishu/Journal of Propulsion Technology, **44**, *5*, pp. 2859-2865 (2023).
29. B. Agrawal, R. Sharma, R.K. Khanna, *A novel design of triangular-shaped hexagonal fractal antenna for satellite communication*, International Journal of Advanced Technology and Engineering Exploration, **10**, *99*, pp. 232–239 (2023).
30. R.K. Saraswat, M. Kumar*, Design and implementation of a multiband metamaterial-loaded reconfigurable antenna for wireless applications,* International Journal of Antennas and Propagation, **2021**, pp. 1–21 (2021).
31. S. Mallikharjuna Rao, T. Setty Vennela Srujana, G.B. Bindu, *Design and analysis of reconfigurable antenna for wide band applications*, In Journal of Physics: Conference Series, **2161,** *1*, pp. 012073 (2022).
32. P. Gupta, M. Bharti, A. Kumar, *Circular polarized two-element compact dual-band MIMO antenna for 5G and wearable applications*, Rev. Roum. Sci. Techn. – Électrotechn. Et Énerg., **67,** *3*, pp. 321–326 (2022).